

Analyzing Key Objectives in Human-to-Robot Retargeting for Dexterous Manipulation

Chendong Xin*, Mingrui Yu*, Yongpeng Jiang, Zhefeng Zhang, and Xiang Li†, *Senior Member, IEEE*

Abstract—Kinematic retargeting from human hands to robot hands is essential for transferring dexterity from humans to robots in manipulation teleoperation and imitation learning. However, due to mechanical differences between human and robot hands, completely reproducing human motions on robot hands is impossible. Existing works on retargeting incorporate various optimization objectives, focusing on different aspects of hand configuration. However, the lack of experimental comparative studies leaves the significance and effectiveness of these objectives unclear. This work aims to analyze these retargeting objectives for dexterous manipulation through extensive real-world comparative experiments. Specifically, we propose a comprehensive retargeting objective formulation that integrates intuitively crucial factors appearing in recent approaches. The significance of each factor is evaluated through experimental ablation studies on the full objective in kinematic posture retargeting and real-world teleoperated manipulation tasks. Experimental results and conclusions provide valuable insights for designing more accurate and effective retargeting algorithms for real-world dexterous manipulation. Supplementary materials are available at <https://mingrui-yu.github.io/retargeting>.

Index Terms—Dexterous manipulation, multi-fingered hand, human-to-robot retargeting, teleoperation.

I. INTRODUCTION

TRANSFERRING dexterity from humans to robots is a promising field in dexterous manipulation research, as the complexity of dexterous manipulation tasks poses challenges for classical analytical approaches [1]–[4]. In either collecting robot demonstrations through human teleoperation or learning from offline human manipulations, an essential component is *kinematic retargeting*, which refers to kinematically translating the human hand configuration to robot hand joint positions. One key challenge of retargeting is that, due to the differences in morphology and degrees of freedom (DoFs) between human hands and current robot hands, the human hand configurations can not be exactly reproduced by the robot hand. Consequently, it is inevitable to focus on only partial configuration of the human hand that are more crucial to manipulation tasks when designing the retargeting algorithms.

The most straightforward retargeting approach is direct joint-to-joint mapping, where the robot hand joints follow a

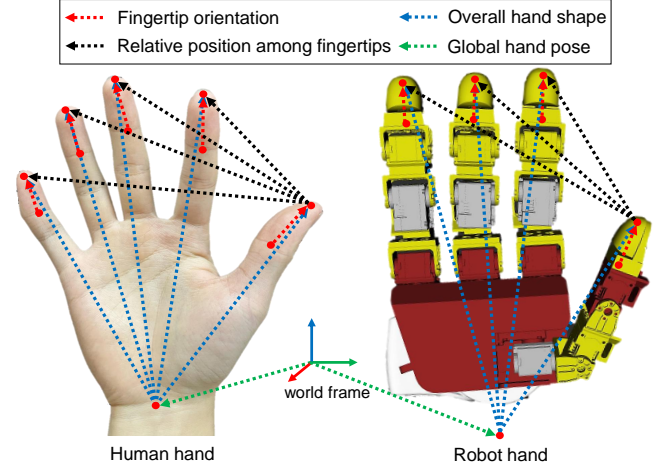


Fig. 1. Crucial objectives in human-to-robot retargeting for dexterous manipulation. This work explores the appropriate formulation of these objectives and experimentally analyzes their significance for different manipulation tasks.

manually defined transformation of the human hand joints [5]–[12]. These approaches require considerable manual efforts to define the joint-space transformation for a certain robot hand. Task-space retargeting is used more widely, which relies on inverse kinematics (IK) solving to determine robot hand joint configuration based on human hand keypoints. The global fingertip position is the fundamental retargeting objective to align human and robot hand in task-space [13]–[17]. In most works, the relative fingertip position to the wrist serves as the retargeting objective [18]–[29]. Distance between two set of vectors from the wrist to the fingertips is minimized to obtain the robot’s optimal joint configurations, thereby preserving the overall hand shape. Some works include finger orientations in the objective to preserve more human-like shapes. The finger shapes are represented in the form of finger bending information by including a set of vectors from palm to middle phalanx [19]. More explicitly, the directions of five proximal phalanges and distal phalanges [30] are used to represent orientations of the finger-roots and fingertips [31]. Additionally, relative position among fingertips can be included to address the challenge of pinch grasps [28], in which a switching weight is used to prioritize the fingers involved in pinching, and the corresponding reference distance on human hand is adjusted to a minimal distance to encourage fingertip contact.

These retargeting approaches have been deployed in real-world manipulation, but they differ in their choices of objectives. Due to the lack of comparative studies, it remains unclear which objectives are more dispensable for which types of manipulation tasks and whether conflicts exist between them.

*Equal contribution.

†Corresponding author: xiangli@tsinghua.edu.cn.

The authors are with the Department of Automation, Beijing National Research Center for Information Science and Technology, Tsinghua University, China. This work was supported in part by the National Key Research and Development Program of China under Grant 2022YFB4701401, in part by National Natural Science Foundation of China under Grant 623B2059 and U21A20517, in part by the BNRist project under Grant BNR2024TD03003, and in part by the Institute for Guo Qiang, Tsinghua University.

A previous survey [32] reviews and classifies the common retargeting methods, but it does not focus on retargeting objectives and not provide experimental evaluations.

This work aims to analyze the key objectives in retargeting for dexterous manipulation through experimental comparison. We summarize objectives that are used in recent research on dexterous retargeting and propose a comprehensive retargeting objective formulation that considers all intuitively crucial factors illustrated in Fig. 1. By conducting ablation studies on the full objective in kinematic posture retargeting and real-world manipulation teleoperation, we analyze the significance and effectiveness of different objectives in different tasks. The experimental results and conclusions provide valuable insights for future research on designing retargeting algorithms for learning dexterous manipulation from humans or teleoperation.

II. METHOD

We intuitively list the factors that are potentially crucial to human-to-robot retargeting for dexterous manipulation:

- **Global hand pose:** the robot's hand pose in the global frame should be aligned with the human's in dexterous manipulation involving large arm motions.
- **Overall hand shape:** the robot hand should replicate a similar overall hand shape to the human hand to achieve similar postures.
- **Relative position among fingertips:** the spatial relationship among each fingertip (e.g., thumb and index) is critical for manipulation tasks that require precise coordination of fingertips.
- **Fingertip orientations:** the accurate fingertip orientations ensure appropriate directions of contact normals during contact-rich dexterous manipulation.

Based on the intuitive factors above, we formulate their corresponding mathematical representations and construct a complete retargeting objective.

Global hand pose: The global hand pose is typically formulated with a wrist position term $\mathcal{L}_{\text{wrist_pos}}$ and a wrist orientation term $\mathcal{L}_{\text{wrist_rot}}$. However, accurate tracking of global wrist pose is not necessary in most dexterous manipulation tasks and may reduce accuracy in fingertip positions. Due to different hand morphologies between the human and robot, the fingertip positions relative to the wrist may conflict with the relative positions between fingertips and fingertip orientations. As a result, it can be better to allow adjustment of the wrist pose in exchange for higher fingertip accuracy. Specifically, we replace the wrist position objective with a thumb-tip position objective $\mathcal{L}_{\text{thumb_pos}}$ and apply joint optimization of the arm-hand joint positions. The retargeted wrist orientation is regularized through the wrist orientation objective $\mathcal{L}_{\text{wrist_rot}}$ with a relatively small weight. The complete term is formulated as:

$$\mathcal{L}_{\text{hand_pose}} = \|\mathbf{p}_{\text{thumb}}^h - \mathbf{p}_{\text{thumb}}^r\|_2^2 + \beta_{\text{rot}} \text{angle}(\mathbf{q}_{\text{wrist}}^h, \mathbf{q}_{\text{wrist}}^r), \quad (1)$$

where $\mathbf{p}_{\text{thumb}}$ is the thumb fingertip position of human and robot, and $\mathbf{q}_{\text{wrist}}$ is the orientation of human and robot wrist.

Overall hand shape: The overall hand shape is represented by the fingertip positions relative to the wrist position. The fingertip position term $\mathcal{L}_{\text{fingertip_pos}}$ measures the difference in

a set of vectors defined from the wrist to the fingertips of the robot and human hand:

$$\mathcal{L}_{\text{fingertip_pos}} = \sum_{i=1}^N \|\mathbf{v}_i^h - \mathbf{v}_i^r\|_2^2, \quad (2)$$

where \mathbf{v}_i is the vector from the wrist to the i^{th} fingertip on human and robot hand, and N is the number of fingers. Note that this term needs to be coordinated with the following pinch objective, for which the details are provided in Appendix.

Relative position among fingertips: We use vectors from the thumb to primary fingers (index, middle, ring) to represent the relative positions among fingertips, which is crucial for pinching. We adopt a similar formulation to DexPilot [28] with a switching weight function $s(d_i)$ and a distance rescaling function $l(d_i)$:

$$\mathcal{L}_{\text{pinch}} = \sum_{i=1}^{N-1} s(d_i) \|\gamma_i^r - l(d_i) \hat{\gamma}_i^h\|_2^2, \quad (3)$$

where γ_i is the vector from the thumb fingertip to the fingertip of the i^{th} primary finger, d_i is the length of γ_i and $\hat{\gamma}_i = \frac{\gamma_i}{d_i}$. Instead of using a discrete weight function as [28], we use continuous weight and rescaling functions to ensure smooth transitions. Specifically, our rescaling function linearly rescales human fingertip distances from $[\epsilon_2, \epsilon_1]$ to $[0, \epsilon_1]$. The details are provided in Appendix.

Fingertip orientations: To represent fingertip orientations, we include another set of vectors. In contrast with methods such as DexMV [19] that define the vectors from the wrist to the middle phalanx, our formulation defines the vectors from the distal interphalangeal (DIP) joints to the fingertips, which represent fingertip orientations more directly:

$$\mathcal{L}_{\text{fingertip_rot}} = \sum_{i=1}^N \|\mathbf{r}_i^h - \mathbf{r}_i^r\|_2^2, \quad (4)$$

where \mathbf{r}_i is the vector from the DIP joint to the fingertip.

The final retargeting optimization objective considering all the above factors can be specified as:

$$\mathcal{L}_{\text{total}} = \lambda_1 \mathcal{L}_{\text{thumb_pos}} + \lambda_2 \mathcal{L}_{\text{wrist_rot}} + \lambda_3 \mathcal{L}_{\text{fingertip_pos}} + \lambda_4 \mathcal{L}_{\text{fingertip_rot}} + \lambda_5 \mathcal{L}_{\text{pinch}} + \mathcal{L}_{\text{joint}} + \mathcal{L}_{\text{vel}}, \quad (5)$$

where two joint-space regularization terms are additionally considered. The joint position regularization $\mathcal{L}_{\text{joint}} = \sum_{j=1}^m w_j^{\text{pos}} \|q_j - \bar{q}_j\|_2^2$ penalizes the deviation of some joints from a pre-defined joint configuration \bar{q} . The joint velocity regularization $\mathcal{L}_{\text{vel}} = \sum_{j=1}^m w_j^{\text{vel}} \|q_j - q_j^{\text{prev}}\|_2^2$ penalizes large changes in joint positions compared to previous timestep to encourage trajectory smoothness.

III. EVALUATIONS AND RESULTS

A. Evaluation Setup

Implementation: Simulation studies involve a Leap Hand [33] and a shadow hand, both mounted on a Franka Emika Panda arm. Real-world experiments are conducted on a teleoperation system with a Leap Hand, a Panda arm, and an Apple Vision Pro for human hand detection [34]. The retargeting

TABLE I
DEFINITION OF THE ABLATIONS FOR COMPARATIVE STUDIES.

Category	Ablation	Definition
Full	Full	Complete retargeting objective $\mathcal{L}_{\text{total}}$ with all terms (5)
Fingertip pinch	A1	Remove the pinch term $\mathcal{L}_{\text{pinch}}$ (6)
	A2	Use actual pinch distance without distance rescaling in (6)
Fingertip orientation	A3	Remove the fingertip orientation term $\mathcal{L}_{\text{fingertip_rot}}$ (4)
	A4	Replace the vectors from DIP joints to fingertips with vectors from the wrist to DIP joints in (4)
Global wrist pose	A5	Replace the thumb position term in (1) with a wrist position term
	A6	Replace the thumb position term in (1) with a wrist position term and remove $\mathcal{L}_{\text{pinch}}$ and $\mathcal{L}_{\text{fingertip_rot}}$
Joint regularization	A7	Remove the joint position regularization $\mathcal{L}_{\text{joint}}$
	A8	Replace the thumb position term in (1) with a wrist position term and remove $\mathcal{L}_{\text{pinch}}$, $\mathcal{L}_{\text{fingertip_rot}}$, and $\mathcal{L}_{\text{joint}}$

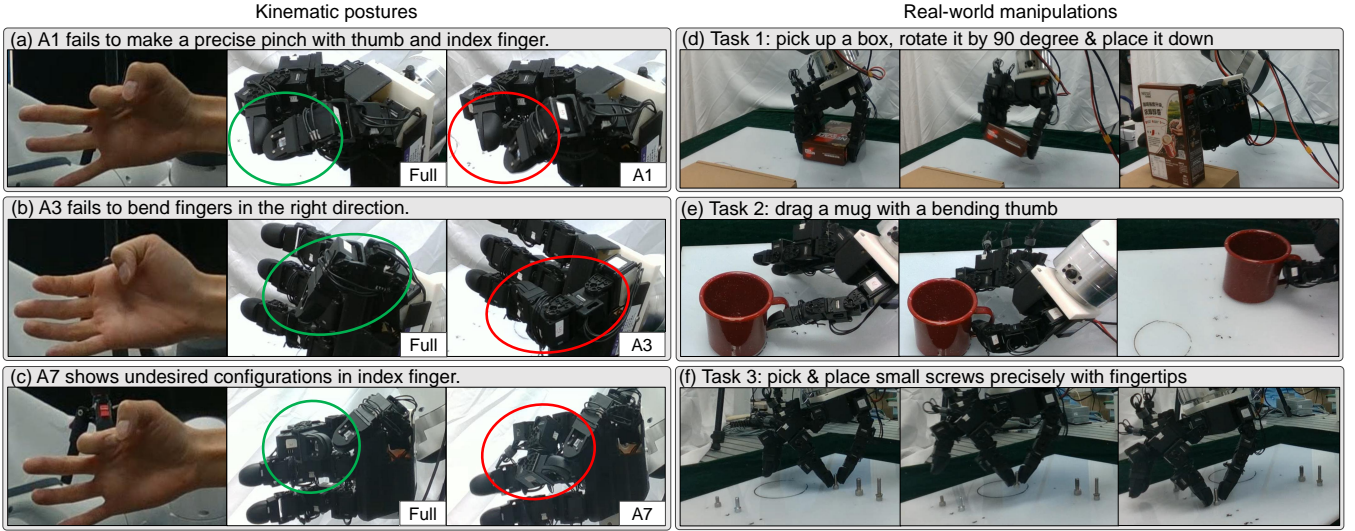


Fig. 2. Snapshots of the real-world kinematic postures retargeting (left) and the three manipulation tasks (right). (a) to (c): each row shows a human hand posture and the corresponding retargeted robot postures using the full objective and an ablation implementation. (d) to (e): each row shows the snapshots of the manipulation process of one task using the full retargeting objective.

objective is optimized in real time using the Sequential Least-Squares Quadratic Programming in the NLOpt library [35].

Ablation setup: To analyze the significance of each retargeting objective, we implement ablations by removing or changing certain objective terms in $\mathcal{L}_{\text{total}}$ (5). The detail of the ablation setup is described in Table I.

Kinematic posture retargeting tasks: We evaluate the full retargeting objective and eight ablations across offline data of three pinch motions involving the thumb and the index, middle, and ring fingers, respectively. We use four quantitative metrics for kinematic postures: 1) average fingertip position error in the global frame, 2) average fingertip position error relative to the wrist, 3) average fingertip position error relative to the thumb, and 4) average fingertip orientation error. The results on Leap Hand are shown in Fig. 3. The results on another trajectory involving finger crossing motions and results on Shadow Hand are provided in the Appendix. The snapshots of posture retargeting in the real world are shown in Fig. 2.

Real-world manipulation tasks: We design three representative real-world manipulation teleoperation tasks :

- 1) Pick up a box, rotate it by 90 degrees, and place it down, which represents commonly used pick-and-place tasks in dexterous teleoperation.
- 2) Drag a mug through its handle using the bent thumb, where fingertip orientation plays a decisive role.
- 3) Pick up five upright-standing screws of different sizes and place them on target positions vertically, where precise pinches are important.

For each task, we sequentially evaluate the full retargeting objective and the seven ablations (A1 to A7), and repeat the entire sequence three times. The above tests are conducted twice with two human pilots. For task 1 and 2, we use mean completion time to assess performance of pilots, as all trials are successful. For task 3, we use success rate for comparison. The manipulation results are summarized in Fig. 4.

B. Analysis of Results

We analyze the results of kinematic posture retargeting and real-world manipulations in *four perspectives* corresponding to the designed objectives.

Fingertip pinch: A1 and A2 are the ablation of fingertip pinch term. The results show that: 1) removing the pinch term in A1 results in significantly higher errors in both fingertip position and relative position to the thumb (A1 in Fig. 3). This results from the potential conflict between the global fingertip position and the fingertip position relative to the wrist, due to

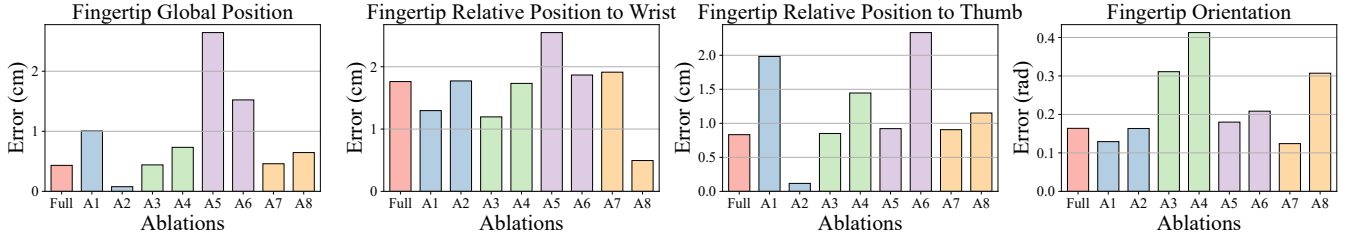


Fig. 3. Results of kinematic posture retargeting on finger pinch trajectories. Each bar shows the error of one ablation implementation and the colors represent the ablation category defined in Table I. For the metrics of fingertip global position and fingertip relative position to the thumb, only the errors of the two fingers involved in the pinching motion are considered.

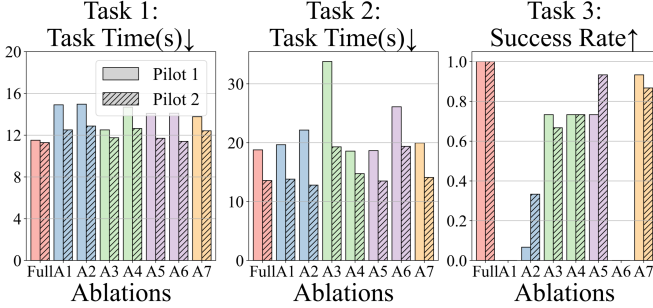


Fig. 4. Results of the real-world manipulations. Task 1 and 2 are assessed by task time, while Task 3 is evaluated by success rate. Each pair of bars shows the error of one ablation implementation and the colors represent the ablation category defined in Table I. The two pilots are distinguished by hatched bars.

different hand morphologies between the human and robot; 2) in real-world manipulations, removing the pinch term in A1 leads to failure in tasks involving pinch motions, as it cannot close the gap between thumb and index fingertips (A1 in Task 3, Fig. 4). This is also displayed in posture (a) in Fig. 2; 3) using actual pinch distances without rescaling in A2 results in minimal error in both metrics (A2 in Fig. 3), but could lead to low success rate in real-world manipulation tasks, primarily due to that using actual pinch distance is vulnerable to human finger tracking inaccuracy (A2 in Task 3, Fig. 4).

Fingertip orientations: A3 and A4 correspond to the ablation of fingertip orientation term. The results suggest: 1) DIP-to-tip vectors hold more explicit information of fingertip orientation than wrist-to-DIP vectors. Replacing the DIP-to-tip vectors with wrist-to-DIP vectors shows little advantage in fingertip orientation error over no orientation consideration (A4 in Fig. 3), as the DIP-to-tip vectors may be changed by fingertip relative position terms even though the wrist-to-DIP vectors are fixed; 2) in real-world manipulation Task 2, no consideration of fingertip orientations results in poor performance as the robot hand fails to replicate the finger bending motion of the human pilots to hook the mug handle (A3 in Task 2, Fig. 4). In addition, it may occur that the finger bends in a wrong direction like posture (b) in Fig. 2; and 3) the missing of fingertip orientation information can also have negative impacts on precise manipulation tasks such as task 3, as inaccuracy in orientation leads to undesired contact normals with the object (A3 in Task 3, Fig. 4).

Global hand pose: A5 and A6 are the ablation of global hand pose. The results show that: 1) determining the global hand pose by the thumb fingertip position term instead of wrist

position term leads to a significantly lower error in fingertip global position (A5 in Fig. 3), primarily due to that using the thumb position term sacrifices in wrist position accuracy in exchange for better alignment of fingertips; 2) when using the exact wrist pose, removing the pinch term also leads to higher errors in fingertip relative position to the thumb (A6 in Fig. 3), and removing the fingertip orientation term hampers finger bending (A6 in Task 2 in Fig. 4); 3) in real-world tasks, the choice of thumb fingertip position term and wrist position term does not bring up much difference (A5 in Fig. 4), because human pilots can easily adjust the global hand position to eliminate the influence of fingertip global position inaccuracy.

Joint position regularization: A7 and A8 removes the joint position regularization term. The corresponding results suggest that: 1) from the comparison between full and A7 in Fig. 3, joint position regularization term seems to have little impact in both simulation and real-world manipulation. However, without this term, it may occur that the hand displays undesired joint configurations like posture (c) in Fig. 2. The joint position regularization makes the retargeting result more truthful without negative impacts; 2) the comparison of A8 and A6 shows that when using wrist position term for global hand pose, the joint position regularization term adds to the errors in fingertip global position and relative position to the wrist and the thumb (A8 in Fig. 3). In contrast, when using thumb fingertip position, the joint position regularization term has little impact on position errors.

IV. CONCLUSION

This work analyzes the significance of different objectives in human-to-robot retargeting for dexterous manipulation through both kinematic posture retargeting and three representative real-world manipulation tasks. The comprehensive results demonstrate that 1) the fingertip pinch objective is crucial for manipulation tasks involving precise fingertip coordination; 2) the fingertip orientation objective should be included for tasks sensitive to finger orientation rather than solely position; 3) allowing wrist pose adjustment instead of using exact human wrist pose benefits the accuracy of fingertip poses; 4) joint position regularization makes the retargeting postures appear more natural while having negligible negative impacts; and 5) all terms using the proposed formulation do not demonstrate conflicts and perform well in all tasks. We believe this study provides valuable insight for designing retargeting algorithms in future work on learning dexterous manipulation from humans or dexterous teleoperation.

TABLE II
DESCRIPTIONS OF SUPPLEMENTARY MATERIALS

Supplementary material	Description
Project website	https://mingrui-yu.github.io/retargeting
Appendix	Supplementary results and implementation details are provided in Appendix, which includes hyper-parameters of the retargeting algorithm, the detailed formulation of the pinch objective, and additional quantitative results of kinematic posture retargeting on another trajectory involving finger crossing motions and on the Shadow Hand. The appendix is also available on the project website .
Video	The video of the real-world experiments is available on the project website , which demonstrates the real-world kinematic posture retargeting, three real-world manipulation tasks for evaluation, and additional trials on manipulation tasks of higher complexity.
Source code	The code is open-sourced on the project website (GitHub), which includes the implementation of the retargeting algorithm and the evaluation on kinematic postures in simulation. We provide a detailed guideline for setting up everything and to launch the evaluation. Users are encouraged to report issues via GitHub.
Dataset	All human hand motion trajectories recorded by Apple Vision Pro in this study are provided on the project website . The format of the dataset is described by the instructions in the corresponding README file.
CAD files	The CAD files of the fingertips and the URDF of the whole robot (i.e., Panda arm + Leap Hand + fingertips) are provided on the project website .

REFERENCES

- [1] T. Pang, H. T. Suh, L. Yang, and R. Tedrake, "Global planning for contact-rich manipulation via local smoothing of quasi-dynamic contact models," *IEEE Trans. Robot.*, 2023.
- [2] Y. Jiang, M. Yu, X. Zhu, M. Tomizuka, and X. Li, "Contact-implicit model predictive control for dexterous in-hand manipulation: A long-horizon and robust approach," in *2024 IEEE/RSJ International Conference on Intelligent Robots and Systems (IROS)*, 2024, pp. 5260–5266.
- [3] M. Yu, Y. Jiang, C. Chen, Y. Jia, and X. Li, "Robotic in-hand manipulation for large-range precise object movement: The rgmc champion solution," *IEEE Robotics and Automation Letters*, 2025.
- [4] M. Yu, B. Liang, X. Zhang, X. Zhu, L. Sun, C. Wang, S. Song, X. Li, and M. Tomizuka, "In-hand following of deformable linear objects using dexterous fingers with tactile sensing," in *2024 IEEE/RSJ International Conference on Intelligent Robots and Systems (IROS)*, 2024, pp. 13 518–13 524.
- [5] Q. Gao, J. Li, Y. Zhu, S. Wang, J. Liufu, and J. Liu, "Hand gesture teleoperation for dexterous manipulators in space station by using monocular hand motion capture," *Acta Astronautica*, vol. 204, pp. 630–639, 2023.
- [6] J. Huang, K. Chen, J. Zhou, X. Lin, P. Abbeel, Q. Dou, and Y. Liu, "Dih-tele: Dexterous in-hand teleoperation framework for learning multiobjects manipulation with tactile sensing," *IEEE/ASME Transactions on Mechatronics*, 2025.
- [7] W. Wei, B. Zhou, B. Fan, M. Du, G. Bao, and S. Cai, "An adaptive hand exoskeleton for teleoperation system," *Chinese Journal of Mechanical Engineering*, vol. 36, no. 1, p. 60, 2023.
- [8] J. Guo, J. Luo, Z. Wei, Y. Hou, Z. Xu, X. Lin, C. Gao, and L. Shao, "Telephantom: A user-friendly teleoperation system with virtual assistance for enhanced effectiveness," *arXiv preprint arXiv:2412.13548*, 2024.
- [9] M. V. Liarokapis, P. K. Artemiadis, and K. J. Kyriakopoulos, "Telemanipulation with the dlr/hit ii robot hand using a dataglove and a low cost force feedback device," in *21st Mediterranean Conference on Control and Automation*, 2013, pp. 431–436.
- [10] G. Giudici, B. Omarali, A. A. Bonzini, K. Althoefer, I. Farkhatdinov, and L. Jamone, "Feeling good: Validation of bilateral tactile telemanipulation for a dexterous robot," in *Annual Conference Towards Autonomous Robotic Systems*. Springer, 2023, pp. 443–454.
- [11] S. P. Arunachalam, I. Güzey, S. Chintala, and L. Pinto, "Holo-dex: Teaching dexterity with immersive mixed reality," in *2023 IEEE International Conference on Robotics and Automation (ICRA)*, 2023, pp. 5962–5969.
- [12] A. Iyer, Z. Peng, Y. Dai, I. Guzey, S. Haldar, S. Chintala, and L. Pinto, "Open teach: A versatile teleoperation system for robotic manipulation," *arXiv preprint arXiv:2403.07870*, 2024.
- [13] C. Wang, H. Shi, W. Wang, R. Zhang, L. Fei-Fei, and C. K. Liu, "Dex-cap: Scalable and portable mocap data collection system for dexterous manipulation," in *Robotics: Science and Systems (RSS)*, 2024.
- [14] K. Shaw, Y. Li, J. Yang, M. K. Srirama, R. Liu, H. Xiong, R. Mendonca, and D. Pathak, "Bimanual dexterity for complex tasks," *arXiv preprint arXiv:2411.13677*, 2024.
- [15] H. Zhang, S. Hu, Z. Yuan, and H. Xu, "Doglove: Dexterous manipulation with a low-cost open-source haptic force feedback glove," *arXiv preprint arXiv:2502.07730*, 2025.
- [16] S. P. Arunachalam, S. Silwal, B. Evans, and L. Pinto, "Dexterous imitation made easy: A learning-based framework for efficient dexterous manipulation," in *2023 IEEE International Conference on Robotics and Automation (ICRA)*, 2023, pp. 5954–5961.
- [17] S. Chen, C. Wang, K. Nguyen, L. Fei-Fei, and C. K. Liu, "Arcap: Collecting high-quality human demonstrations for robot learning with augmented reality feedback," *arXiv preprint arXiv:2410.08464*, 2024.
- [18] D. Antotsiou, G. Garcia-Hernando, and T.-K. Kim, "Task-oriented hand motion retargeting for dexterous manipulation imitation," in *Proceedings of the European conference on computer vision (ECCV) workshops*, 2018, pp. 0–0.
- [19] Y. Qin, Y.-H. Wu, S. Liu, H. Jiang, R. Yang, Y. Fu, and X. Wang, "Dexmv: Imitation learning for dexterous manipulation from human videos," in *European Conference on Computer Vision*. Springer, 2022, pp. 570–587.
- [20] Y. Qin, W. Yang, B. Huang, K. Van Wyk, H. Su, X. Wang, Y.-W. Chao, and D. Fox, "Anyteleop: A general vision-based dexterous robot arm-hand teleoperation system," *arXiv preprint arXiv:2307.04577*, 2023.
- [21] R. Ding, Y. Qin, J. Zhu, C. Jia, S. Yang, R. Yang, X. Qi, and X. Wang, "Bunny-visionpro: Real-time bimanual dexterous teleoperation for imitation learning," *arXiv preprint arXiv:2407.03162*, 2024.
- [22] S. Yang, M. Liu, Y. Qin, R. Ding, J. Li, X. Cheng, R. Yang, S. Yi, and X. Wang, "Ace: A cross-platform visual-exoskeletons system for low-cost dexterous teleoperation," *arXiv preprint arXiv:2408.11805*, 2024.
- [23] S. Huang, Z. Zhang, M. Chen, Z. Wu, Q. Li, and Z. Ming, "Designing of a dexterous hand and performance evaluation based on teleoperation," in *2024 International Conference on Intelligent Robotics and Automatic Control (IRAC)*, 2024, pp. 169–172.
- [24] K. Shaw, S. Bahl, A. Sivakumar, A. Kannan, and D. Pathak, "Learning dexterity from human hand motion in internet videos," *The International Journal of Robotics Research*, vol. 43, no. 4, pp. 513–532, 2024.
- [25] H. Yuan, B. Zhou, Y. Fu, and Z. Lu, "Cross-embodiment dexterous grasping with reinforcement learning," *arXiv preprint arXiv:2410.02479*, 2024.
- [26] X. Cheng, J. Li, S. Yang, G. Yang, and X. Wang, "Open-television: Teleoperation with immersive active visual feedback," *arXiv preprint arXiv:2407.01512*, 2024.
- [27] B. Romero, H.-S. Fang, P. Agrawal, and E. Adelson, "Eyesight hand: Design of a fully-actuated dexterous robot hand with integrated vision-based tactile sensors and compliant actuation," in *2024 IEEE/RSJ International Conference on Intelligent Robots and Systems (IROS)*, 2024, pp. 1853–1860.
- [28] A. Handa, K. Van Wyk, W. Yang, J. Liang, Y.-W. Chao, Q. Wan, S. Birchfield, N. Ratliff, and D. Fox, "Dexpilot: Vision-based teleoperation of dexterous robotic hand-arm system," in *2020 IEEE International Conference on Robotics and Automation (ICRA)*, 2020, pp. 9164–9170.
- [29] A. Sivakumar, K. Shaw, and D. Pathak, "Robotic telekinesis: Learning a robotic hand imitator by watching humans on youtube," in *Robotics: Science and Systems*, 2022.
- [30] Wikipedia contributors, "Phalanx bone — Wikipedia, the free encyclopedia," https://en.wikipedia.org/w/index.php?title=Phalanx_bone&oldid=1275529475, 2025, [Online; accessed 1-April-2025].
- [31] S. Li, X. Ma, H. Liang, M. Görner, P. Ruppel, B. Fang, F. Sun, and J. Zhang, "Vision-based teleoperation of shadow dexterous hand using end-to-end deep neural network," in *2019 International Conference on Robotics and Automation (ICRA)*, 2019, pp. 416–422.
- [32] R. Meattini, R. Suarez, G. Palli, and C. Melchiorri, "Human to robot hand motion mapping methods: Review and classification," *IEEE Transactions on Robotics*, vol. 39, no. 2, pp. 842–861, 2022.
- [33] K. Shaw, A. Agarwal, and D. Pathak, "LEAP Hand: Low-cost, efficient, and anthropomorphic hand for robot learning," *Robotics: Science and Systems (RSS)*, 2023.
- [34] Y. Park and P. Agrawal, "Using apple vision pro to train and control robots," 2024. [Online]. Available: <https://github.com/Improbable-AI/VisionProTeleop>
- [35] S. G. Johnson, "The NLOpt nonlinear-optimization package," <https://github.com/stevengi/nlopt>, 2007.

APPENDIX

ADDITIONAL KINEMATIC POSTURE RETARGETING RESULTS

Three sets of additional quantitative results of kinematic posture retargeting on another trajectory involving finger crossing motions and on the Shadow Hand are shown in Fig. 5. Similar conclusions to the main text can be derived.

ADDITIONAL DETAILS OF OBJECTIVE FORMULATION

Relative position among fingertips: The pinch term is formulated as:

$$\mathcal{L}_{\text{pinch}} = \sum_{i=1}^{N-1} s(d_i) \|\gamma_i^r - l(d_i) \hat{\gamma}_i^h\|^2, \quad (6)$$

where γ_i is the vector from the thumb fingertip to the fingertip of the i^{th} primary finger, $d_i = \|\gamma_i^h\|$ and $\hat{\gamma}_i^h = \frac{\gamma_i^h}{d_i}$. Instead of using a discrete weight function as DexPilot, we use a continuous weight function

$$s(d_i) = \text{sigmoid}(d_i, \epsilon_1, 10),$$

where $\text{sigmoid}(\cdot)$ is the sigmoid function defined as follows:

$$\text{sigmoid}(x, c, w) = \frac{1}{1 + e^{w(x-c)}}.$$

Our distance rescaling function is defined as follows:

$$l(d_i) = \begin{cases} 0, & d_i < \epsilon_2 \\ \frac{\epsilon_1 - \epsilon_2}{\epsilon_1 - \epsilon_2} (d_i - \epsilon_2), & \epsilon_2 \leq d_i \leq \epsilon_1 \\ d_i, & d_i > \epsilon_1, \end{cases} \quad (7)$$

where fingertip distance within pinching range $[\epsilon_2, \epsilon_1]$ is linearly rescaled into $[0, \epsilon_1]$. This ensures a continuous transition in the pinching range and avoids sudden changes around the threshold ϵ_1 . In practice we set $\epsilon_1 = 1 \times 10^{-1}$ m and $\epsilon_2 = 1 \times 10^{-2}$ m.

Overall hand shape: To balance fingertip positions relative to the wrist and the thumb, we also set a switching weight for the fingertip position term $\mathcal{L}_{\text{fingertip_pos}}$:

$$\mathcal{L}_{\text{fingertip_pos}} = \sum_{i=1}^N \tilde{s}(d_i) \|\mathbf{v}_i^r - \mathbf{v}_i^h\|^2, \quad (8)$$

where

$$\tilde{s}(d_i) = \text{sigmoid}(d_i, \epsilon_1, -10),$$

so that the sum of $s(d_i)$ and $\tilde{s}(d_i)$ will be a fixed number. In ablation studies where the pinch term is removed (A1, A6 and A8), we set $\tilde{s}(d_i)$ to be a constant 1.0 as in (2).

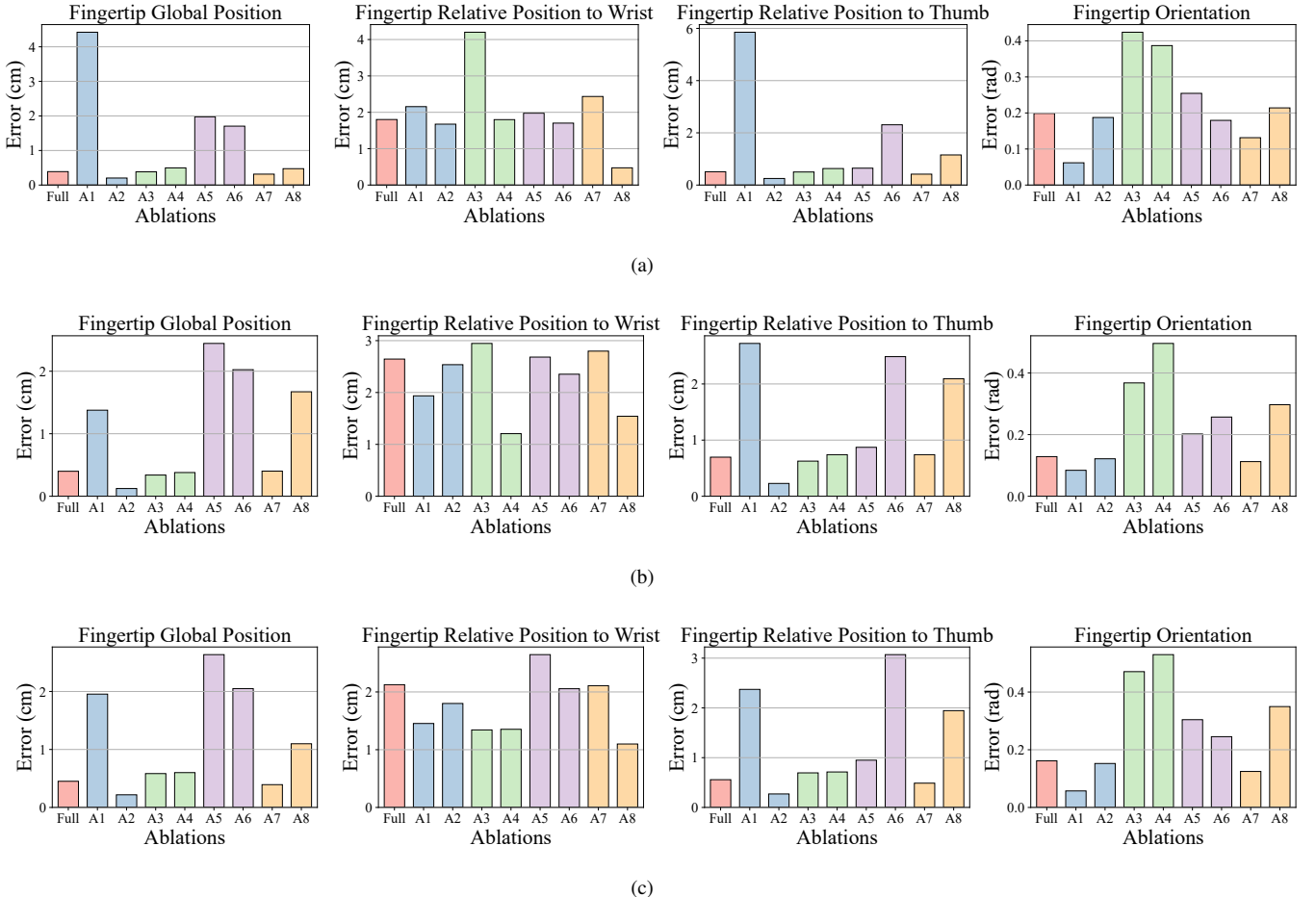


Fig. 5. Additional results on kinematic posture Retargeting. (a) Kinematic posture retargeting results using Leap hand on another trajectory involving finger crossing motion. (b) Kinematic posture retargeting results using Shadow hand on the same pinch motion trajectory as in the main text. (c) Kinematic posture retargeting results using Shadow hand on the trajectory involving finger crossing motion.

IMPLEMENTATION

The hyper-parameters used in the retargeting objective are listed in Table III.

TABLE III
HYPER-PARAMETERS

Hyper Parameter	Value
λ_1	10
λ_2	0.1
λ_3	1
λ_4	10
λ_5	10
w_j^{pos} (Leap hand)	0.5, $j = 7, 11, 15, 18$ 0.1, $j = 20$ 0, else
w_j^{pos} (Shadow Hand)	0.5, $j = 9, 13, 17, 22$ 0.1, $j = 26$ 0, else
w_j^{vel} (Leap hand)	0.1, $j = 0 \sim 6$ 0.01, $j = 7 \sim 22$
w_j^{vel} (Shadow Hand)	0.1, $j = 0 \sim 6$ 0.01, $j = 7 \sim 30$

A relatively small weight of 0.1 is assigned to the wrist orientation term (λ_2), as the objective aims to emphasize fingertip tracking accuracy rather than wrist pose accuracy.

For the weights of joint position and velocity regularization terms w_j^{joint} and w_j^{vel} , index j from 0 to 6 corresponds to the joints of the Panda arm, while indices $j = 7$ to 22 and $j = 7$ to 30 correspond to the joints of the Leap hand and the Shadow Hand respectively. Note that here we assume all DoFs of the Shadow Hand are actuated. For Leap hand, $j = 7, 11, 15$ correspond to the abduction/adduction joints of index, middle and ring, $j = 18$ corresponds to the DIP joint of the ring, and $j = 20$ corresponds to the rotation of the thumb. For Shadow Hand, $j = 9, 13, 17, 22$ correspond to the finger movements of index, middle, ring and little finger in the palm plane, while $j = 26$ corresponds to the rotation of the thumb. For joints with non-zero position regularization, the pre-defined joint configurations are set to $\bar{q}_j = 0$.

In our implementation, we rescale the size of the human hand by a factor of 1.5 for the Leap hand and 1.0 for the Shadow Hand to address the size difference between human and robot hand. In the real-world experiments, the retargeting control frequency is 20 Hz, and we use an exponential moving average with $\alpha_{\text{ema}} = 0.3$ to further smoothen the joint movements:

$$\mathbf{q}_t = \alpha_{\text{ema}} \cdot \mathbf{q}_t + (1 - \alpha_{\text{ema}}) \cdot \mathbf{q}_{t-1} \quad (9)$$